Articles

Crystallization of $LnCu_2O_4$ (Ln = La, Nd, Sm, Eu, Gd, Dy, Ho, Y, Er) from Hydroxide Melts: Synthesis and Structure

Jeanne L. Luce and Angelica M. Stacy*

Department of Chemistry, University of California at Berkeley, Berkeley, California, 94720-9989

Received April 12, 1996. Revised Manuscript Received January 17, 1997[⊗]

The synthesis and structure of $LnCu_2O_4$ with Ln = La, Nd, Sm, Eu, Gd, Dy, Ho, Y, and Er are reported. These cuprates were synthesized by precipitation from NaOH/KOH at 350−400 °C under ambient conditions. The effects of changing the relative amounts of NaOH and KOH, the quantities of the starting reagents, the reaction temperature, and the time at which the reagents were added on the yield, purity, and crystallinity of $LnCu_2O_4$ are described. Generally, the formation of $LnCu_2O_4$ is favored in dry, highly oxidizing melts with large quantities of dissolved reactants. Powder X-ray diffraction data were used to refine the structure of the various analogues using Rietveld profile analysis. The lattice parameters and average Ln−O distances decrease with decreasing size of the lanthanide ion. The average Cu−O bond distances, on the other hand, do not significantly change with the size of the lanthanide ion.

Introduction

The synthesis of a new family of cuprate phases, $LnCu_2O_4$, with a unique structure-type has been reported recently.[1,2] Keller et al. found that several members of this family of cuprates (Ln = La, Nd, Sm, Eu) can be precipitated from molten NaOH at 350−400 °C under ambient conditions,[1] and Chen et al. reported the preparation of several members (Ln = Nd, Gd, Y, Er, Lu) by direct reaction of Ln_2O_3 and CuO at 1000−1200 °C under elevated oxygen pressures (40−100 kbar).[2] These phases crystallize in a new structure-type in which planar CuO_4 units are corner-shared in a three-dimensional array as shown in Figure 1. The copper is in an average formal oxidation state of 2.5+, and the magnetic properties are unusual and complex.[1] Further studies of the magnetism depend on the availability of large quantities of sample of suitable purity and crystallinity for powder neutron diffraction studies. In this paper, we show how to control the reaction environment in the molten hydroxide synthesis in order to optimize the yield and crystallinity of these cuprate phases and also extend the series to include additional lanthanide elements.

Precipitation from molten alkali-metal hydroxides is a versatile means by which to synthesize a number of cuprates with a variety of formal copper oxidation states (e.g., $La_{2-x}Na_xCuO_4$,[3] $NdBa_2Cu_4O_8$,[4] $LiBa_4CuO_4(CO_3)_2$[5]). This synthetic route involves first establishing conditions that allow for the dissolution of starting reagents (typically metal oxides) and subsequently modifying the reaction conditions to crystallize the desired oxide phase. The use of molten hydroxides as a solvent allows for product formation at significantly lower temperatures and/or oxygen pressures compared with those required for direct reaction of the solid reactants. Specifically for the case of $LnCu_2O_4$, while elevated temperatures and oxygen pressures are required for the solid-state reaction, these phases can be formed at much lower temperatures and under ambient conditions by precipitation from molten hydroxides.

To obtain a desired product by precipitation from molten hydroxides, a number of interdependent reaction variables must be controlled. For example, the same melt which was used to produce $LnCu_2O_4$ can be used to produce Ln_2CuO_4 under slightly different conditions.[3] To optimize the yield, purity, and crystallinity of the $LnCu_2O_4$ product, reactant quantities, reaction temperature, atmosphere over the melt, and time of addition of the reactants must be selected carefully. Moreover, because of variations in solubility of Ln_2O_3 and the different effects of dissolved Ln^{3+} on the melt chemistry, the synthesis parameters vary with the lanthanide element. Here we report conditions that allowed for the precipitation of additional members of the $LnCu_2O_4$ family of cuprates with Ln = Gd, Dy, Ho, Y, and Er from

* To whom correspondence should be addressed.

[⊗] Abstract published in *Advance ACS Abstracts,* March 1, 1997.

(1) Keller, S. W.; Carlson, V. A.; Sandford, D.; Stenzel, F.; Stacy, A. M.; Kwei, G. H.; Alario-Franco, M. *J. Am. Chem. Soc.* **1994**, *116*, 8070.

(2) Chen, B.-H.; Walker, D.; Suard, E. Y.; Scott, B. A. *Chem. Mater.* **1995**, *7*, 355.

(3) Stoll, S. L.; Stacy, A.; M.; Torardi, C. C. *Inorg. Chem.* **1994**, *33*, 2761

(4) Sandford, D. W.; Marquez, L. N.; Stacy, A. M. *Appl. Phys. Lett.* **1995**, *67*, 422.

(5) VerNooy, P. D.; Stacy, A. M. *J. Solid State Chem.* **1991**, *95*, 270.

S0897-4756(96)00226-8 CCC: $14.00

Structure of $LnCu_2O_4$

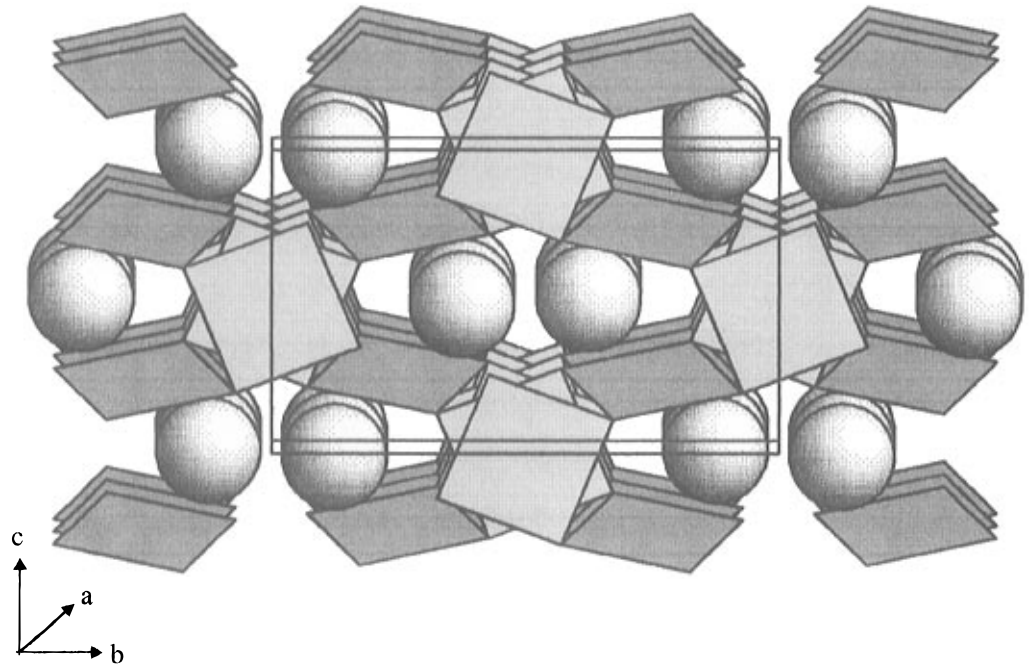

Figure 1. Bravais unit cell of $LnCu_2O_4$ is framed by the box. Ln atoms are depicted as balls. The dark gray squares represent $Cu(1)O_4$ units; the light gray squares represent $Cu(2)O_4$ units.

molten NaOH/KOH melts at 350−400 °C, as well as conditions that resulted in improved yields and crystallinity for Ln = La, Nd, Sm, and Eu.

In addition, the structures of the various members of the $LnCu_2O_4$ family were determined by Rietveld profile refinement of powder X-ray diffraction data. In these phases, there are two crystallographically distinct sites for Cu, one with Cu−O bond distances typical of Cu^{2+} and one with bond distances typical of Cu^{3+}, as determined for $NdCu_2O_4$ by powder neutron diffraction.[1] As the lanthanide series is traversed, the volume of the unit cell shrinks due to the decreasing size of the lanthanide ion. The effects of this volume decrease on the average Ln−O and Cu−O bond lengths are reported below.

Experimental Section

Synthesis. The melt used for the preparation of $LnCu_2O_4$ consisted of NaOH and/or KOH (both A.C.S. reagent grade and purchased from Fisher Scientific). The reactant containing Cu was CuO (Aldrich 99%). For the rare earth, Ln_2O_3 was used (these were at least 99.9% pure and from one of the following sources: Aldrich, Cerac, Fluka, Rare Earth Products, Alfa, Strem, REacton).[6] Where stated, reagents were dried overnight at 200 °C before use; otherwise, the reagents were used as purchased without further treatment or purification. The reactions were carried out in a silver crucible placed inside an alumina crucible, and both were placed inside a horizontal tube furnace. The silver crucible was cleaned first in 6 M HCl, rinsed, then placed in an ultrasonic cleaner in a beaker containing 12 M NH_4OH, and finally rinsed with water and dried.

(6) In the case of La and Nd, although the reactant bottle was labeled Ln_2O_3, the contents were actually $Ln(OH)_3$ as shown by XRD and TGA.

Table 1. Synthetic Conditions for $LnCu_2O_4$[a]

$LnCu_2O_4$	g of NaOH/g of KOH	molar ratio Na:K	temp (°C)	reaction time (days)	% yield
La	1.4/5.0	1:3	400	1	75
Nd	5.4/6.6	1:1	380	1	85
Sm	5.4/6.6	1:1	380	1	80
Eu	5.4/6.6	1:1	400	1	60
Gd	5.4/6.6	1:1	400	1	65
Dy[b]	2.7/3.3	1:1	400	1	70
Ho	2.7/3.3	1:1	400	7	65
Y	2.7/3.3	1:1	400	7	50
Er	2.7/3.3	1:1	400	14	80
La[c]	11.25/13.75	1:1	400	4	90
Nd[d]	11.25/13.75	1:1	380	4	90
Sm[d]	11.25/13.75	1:1	380	4	75
Eu[d]	11.25/13.75	1:1	400	4	65
Dy[b,d]	11.25/13.75	1:1	400	4	75

[a] Addition of stoichiometric amounts of Ln_2O_3 and CuO after 6 h (1.256 mmol of Cu). [b] Synthesized under flowing wet air. [c] 0.9000 g of CuO (11.32 mmol) used as starting reagent. [d] 1.0000 g of CuO (12.56 mmol) used as starting reagent

As shown in Table 1, several reaction variables were explored: temperature, quantities of reactants, ratio of NaOH to KOH, and the reaction time. In other syntheses, the molar ratio of Ln to Cu as well as the time between heating the melt to the appropriate temperature and adding the reagents (addition time) were also varied. In a typical synthesis, the desired quantities of NaOH and KOH were placed in the silver crucible and into the tube furnace which had been preheated to about 325 °C. The temperature was raised at approximately 100 °C/h to the temperature at which the reaction was to be carried out (approximately 350−400 °C) and held at this temperature for a fixed number of hours (approximately 4−6 h). After this melt pretreatment, the copper and lanthanide reactants were added. For specific reagents, quantities, temperatures, and times, see Table 1.

Upon addition of the copper and lanthanide reagents, the melt turned immediately an opaque blue/black. After heating at the reaction temperature overnight (approximately 16 h), the resulting melt was transparent blue. The rim of the silver crucible had a white crust, which was identified as $K_2CO_3 \cdot 2H_2O$ by powder X-ray diffraction. The melt was quenched to room temperature by removing the crucible from the furnace.

The product was isolated by dissolving the flux in water and then separating the larger $LnCu_2O_4$ crystals from powder impurities. Placing the crucible with water in an ultrasonic cleaner shortened the time required to dissolve the flux significantly. The water turned black, presumably due to the presence of fine impurity particles precipitated upon quenching. Depending on the reaction conditions, these impurity particles consisted of various quantities of Ln_2CuO_4, $Ln(OH)_3$, Ln_2O_3, CuO, Ag, and/or Ag_2O. The water containing the suspended particles was poured out of the crucible carefully in order to isolate the heavier $LnCu_2O_4$ product on the bottom of the crucible. This process was repeated several times until the water in the crucible did not turn cloudy in the ultrasonic cleaner. The polycrystalline sample, consisting of large, shiny, black crystals, was then collected by vacuum filtration and placed in a drying oven at 200 °C for a half hour.

The crucibles were cleaned of crystals of $LnCu_2O_4$ that remained attached to the sides and bottom of the silver crucible by a quick cleaning in 6 M HCl (maximum 5 min) followed by placing the crucible with 12 M NH_4OH in an ultrasonic cleaner for at least 1 h. Occasionally, the crystals were attached too tightly to the silver to be removed with HCl or by scrubbing. In these cases, the crystals were redissolved by heating the crucible with NaOH for at least an hour at 400 °C.

In Table 1, the conditions that gave favorable yields for smaller batches of $LnCu_2O_4$ are listed at the top of the table. Conditions for larger batches of $LaCu_2O_4$ and $NdCu_2O_4$ are given at the bottom of Table 1.

X-ray Diffraction. A Siemens D5000 diffractometer (Cu Kα radiation) was used to analyze the samples. Data were collected in the range $10° \leq 2\theta \leq 100°$ with a step size of 0.01° step and a count time of 5 s. The zero point of the instrument was determined in a separate scan with a LaB_6 standard, and the data were corrected accordingly. All patterns indicated that the samples consisted of a single phase, except for the $DyCu_2O_4$, $HoCu_2O_4$, and $ErCu_2O_4$ analogues which contained a very minor Ln_2O_3 impurity. Representative patterns are given in Figure 2.

The structural parameters of these phases were refined by Rietveld profile analysis with the GSAS software package.[7] No regions of any pattern were excluded during the refinement. The space group and atom positions found in previous refinement of powder neutron diffraction data for $NdCu_2O_4$,[1] as well as lattice parameters calculated with an indexing program (LATPARM[8]), were used as a starting point for the refinement. A five-term Fourier series was used to describe the background. Lattice constants, the scale factor, and the sample shift were refined for all samples. Positions

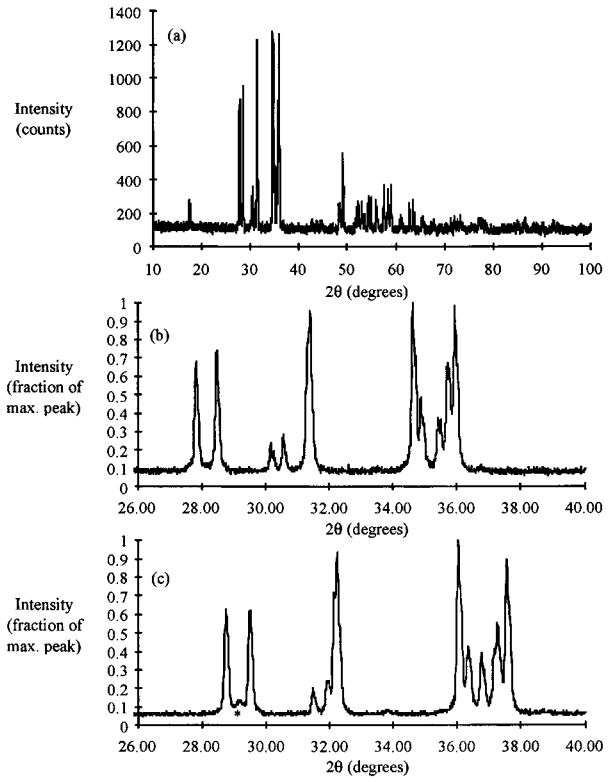

Figure 2. Observed X-ray patterns for $LaCu_2O_4$ (a, b) and $HoCu_2O_4$ (c). Pattern (a) shows the complete pattern for $LaCu_2O_4$. Pattern (b) shows a closeup of $LnCu_2O_4$ in the region where impurity peaks are most likely to occur. None are present. Pattern (c) shows a closeup of the same region for the Ho analogue. A small Ho_2O_3 impurity, its maximum peak indicated by an asterisk, is present.

were refined for the lanthanide (*y* coordinate) and oxygen atoms (all coordinates). (The copper and lanthanide atoms are located on special positions.) Isotropic thermal parameters were refined as indicated. Peak profiles were also refined using a pseudo-Voigtian function, including one symmetric Gaussian term, two symmetric Lorentzian terms, and asymmetric corrections to the Gaussian and Lorentzian terms.

Results and Discussion: Synthesis

There are several advantages of using hydroxide melts for the synthesis of copper oxides generally, and for the synthesis of $LnCu_2O_4$ specifically, over more traditional synthetic techniques. For example, $LnCu_2O_4$ cannot be synthesized by direct reaction of Ln_2O_3 and CuO at elevated temperatures, except at very high oxygen pressures (>40 kbar). In contrast, large quantities of crystalline $LnCu_2O_4$ can be produced rapidly under ambient conditions by precipitation from hydroxide melts, provided a number of reaction variables are controlled properly. The best conditions that we have found for each of the $LnCu_2O_4$ phases are given in Table 1.

The reaction conditions that allow for the synthesis of $LnCu_2O_4$ are those which meet several criteria. First, Ln_2O_3 and CuO must be dissolved, then some of the Cu^{2+} must be oxidized to Cu^{3+}, and finally the solubility product of $LnCu_2O_4$ must be exceeded. Dissolution of oxide reactants and precipitation of $LnCu_2O_4$ requires control over the activity of H_2O, the conjugate acid of OH^-, as well as control over the activities of the

(7) Larson, A. C.; Von Dreele, R. B. Los Alamos Report, LAUR 86-748, 1986, Los Alamos National Laboratory.

(8) Least-squares lattice parameter refinement program obtained from B. Chambers.

dissolved metal ions. The oxidation of Cu^{2+} is dependent on the melt potential which is affected directly by the reaction of O_2 with the melt. Thus, the important reaction variables are those that affect the acid−base chemistry of the melt and the oxidation/reduction chemistry.

The acid−base chemistry of the hydroxide melts can be described by classical Brønsted theory.[9,10] The hydroxide ions of the melt dissociate into H_2O and O^{2-} ions, in much the same way that water in aqueous solutions dissociates into H_3O^+ and OH^- ions:

$$2OH^- \leftrightarrows H_2O(\text{solution}) + O^{2-}(\text{solution}) \quad (1)$$

Thus, melts rich in H_2O are acidic and melts rich in O^{2-} are basic. In general, metal oxides are soluble in acidic and/or basic melts, but not in neutral melts. Alkali-metal hydroxides which have been exposed to air contain a sufficient quantity of water to dissolve Ln_2O_3 and CuO upon melting. Precipitation of metal oxides occurs as H_2O is removed and the activity of O^{2-} is increased. In the experiments described here, removal of H_2O is accomplished primarily by raising the temperature. Key reaction variables include the amounts of reactants and the NaOH/KOH ratio because these can dramatically affect the water content of the melt and the temperature of removal.

The species responsible for the oxidation of metal ions dissolved in molten hydroxides are believed to be superoxides and peroxides produced by reaction of O_2 with the melt as follows:[11]

$$2O^{2-} + O_2 \leftrightarrows 2O_2^{2-} \quad (2)$$

$$O^{2-} + 1.5O_2 \leftrightarrows 2O_2^{-} \quad (3)$$

Since these reactions depend on the O^{2-} ion activity and the partial pressure of O_2 over the melt, the melt potential can be controlled by varying the H_2O content and/or the atmosphere over the melt. We have chosen to fix the atmosphere to ambient conditions and vary the temperature to control the H_2O content. In addition, because the water content varies dramatically during the initial stages of the reaction, we have found that the time at which the reactants are added is an important variable.

In the following three sections, the effects of changing several of the important reaction variables are discussed further. Specifically, the effects of changing the relative amounts of NaOH and KOH, the quantities of the starting reagents, the reaction temperature, and the time at which the reagents containing Cu and La are added on the yield, purity, and crystallinity of $LnCu_2O_4$ are described.

Relative Amounts of Hydroxides. During the course of these investigations, the relative amounts of NaOH and KOH were varied. As shown for $LaCu_2O_4$, $NdCu_2O_4$, and $DyCu_2O_4$ in Table 2, melts richer in KOH produced greater yields of $LnCu_2O_4$. For example, when pure NaOH was used in the synthesis of $LaCu_2O_4$, the yield was negligible. However, by using equal amounts of NaOH and KOH, the yield increased to 55%. The yield increased further with continued increase in the proportion of KOH to about 80% KOH, above which the mixture of hydroxides no longer remained molten at 400 °C. If the reaction temperature was higher than 400 °C, $LaCu_2O_4$ was not formed.

Table 2. Percent Yield versus Relative Amounts of Hydroxides[a]

$LnCu_2O_4$	g NaOH/g KOH	molar ratio Na:K	% yield
La	6/0	1:0	0
	2.7/3.3	1:1	65
	1.4/5.0	1:3	75
	0.5/5.5	1:10	70
Nd	12/0	1:0	0
	5.4/6.6	1:1	85
	0/6[d]	0:1	0
Dy	2.7/3.3	1:1	0
	1.4/5.0	1:3	15
Ho[b]	2.7/3.3	1:1	30
	1.4/5.0	1:3	15
Er[c]	4.3/1.7	3:1	0
	2.7/3.3	1:1	15
	1.4/5.0	1:3	10

[a] Addition of stoichiometric amounts of Ln_2O_3 and CuO after 6 h (1.256 mmol of Cu). Reaction occurred at 400 °C overnight. [b] 4-day reaction time. [c] Reduction at 350 °C for 14 days. [d] Reaction at 450 °C for 1 day.

Although the yields obtained were in general greater in melts richer in KOH, it was not always necessary, or even desirable, to increase the KOH content above the equimolar mixture. For example, as listed in Table 1, several syntheses were carried out in the equimolar melt. For Ln = Nd, Sm, Eu, and Gd, the yields were sufficient (60−85%) with a reaction time of 1 day, and therefore, the effect of increasing the ratio of KOH to NaOH was not explored. For the larger lanthanides (primarily Nd and Sm), there was also increased silver contamination of the product due to etching of the silver crucible when melts richer in KOH were used. In addition, using a melt richer in KOH than equimolar decreased the yield of $HoCu_2O_4$ (see Table 2).

The improved yields of $LnCu_2O_4$ upon increasing the proportion of KOH is most likely due to differences in water content and superoxide content. KOH contains more water than NaOH at a given temperature in the temperature range considered,[12] and therefore, metal oxides are more soluble. Furthermore, it has been shown that the formation of superoxide is more favorable in KOH compared with NaOH,[13] and thus, the oxidation potential of KOH melts is higher. We propose that in melts rich in KOH, the Cu^{2+} is oxidized under conditions that are wet enough to allow for the dissolution of the reactants. In contrast, in NaOH-rich melts, the reactants are not very soluble in the dry melts required for the oxidation of Cu^{2+}, and thus, the yield of $LnCu_2O_4$ is low.

Reactant Quantities. The results of varying the quantities of oxide reactants dissolved in the hydroxide melts are listed in Table 3. In this table, the only variable which was altered was the relative quantities of reactants; this was achieved by changing the amount of hydroxide present or by adding excess CuO. In general, the yield of $LnCu_2O_4$ increased with increasing amounts of reactants relative to hydroxide. This was

(9) Goret, J. *Bull. Soc. Chim.* **1964**, 1074
(10) Doisneau, R. G.; Tremillon, B. *J. Chim. Phys.* **1974**, *71*, 1445.
(11) Lux, H.; Kuhn, R.; Niedermeyer, T. *Z. Anorg. Allg. Chem.* **1959**, *298*, 285.
(12) Tremillion, B.; Doisneau, R. G. *J. Chim. Phys.* **1974**, *71*, 1379.
(13) Greenwood, N. N.; Earnshaw, A. *Chemistry of the Elements*; Pergamon Press: New York, 1984; pp 97, 132.

Table 3. Percent Yield versus Melt Concentration[a]

$LnCu_2O_4$	g of NaOH/ g of KOH	molar ratio Na:K	molar ratio Ln:Cu	mmol of Cu	% yield
La	5.4/6.6	1:1	1:2	1.256	10
	5.4/6.6	1:1	1:4	2.512	30
	2.7/3.3	1:1	1:2	1.256	65
La	1.4/5.0	1:3	1:2	1.256	75
	1.4/5.0	1:3	1:4	2.512	80
Ho[b]	5.4/6.6	1:1	1:2	1.256	15
	2.7/3.3	1:1	1:2	1.256	35
Er[c]	11.25/13.75	1:1	1:2	0.628	0
	2.7/3.3	1:1	1:2	0.628	75

[a] Addition of Ln_2O_3 and CuO after 6 h. Reaction occurred at 400 °C overnight. [b] 4-day reaction time. [c] 14-day reaction time.

especially apparent in the case of $ErCu_2O_4$, where the yield increased from 1% to 75% simply by reducing the volume of the melt. The addition of copper oxide in excess of the 1:2 stoichiometric ratio for Ln to Cu also tended to increase the yields.

We propose that increasing the amounts of oxide reactants increases the yields of $LnCu_2O_4$ because dissolution of the reactants leads to drying of the melt, which in turn leads to quicker precipitation of $LnCu_2O_4$. For example, CuO is dissolved via the following reaction with water in the melt:[14]

$$CuO(solid) + H_2O(solution) \leftrightarrow Cu^{2+}(solution) + 2OH^- \quad (4)$$

The dissolution of oxide results in the removal of water, shifting the melt equilibria to a drier pH_2O. As mentioned previously, two conditions develop as the melt dries: the melt becomes more oxidizing, and metal cations become less soluble. Both conditions favor the formation of $LnCu_2O_4$. The more oxide that dissolves, the quicker these drier conditions are reached, and the faster $LnCu_2O_4$ forms.

Some of the $LnCu_2O_4$ phases formed much faster than others as indicated in Table 1. For example, the Nd, Sm, Eu, and Gd phases formed in reasonable yields overnight in the equimolar melt, but the formation of the La phase required melts richer in KOH. The synthesis of the Dy, Ho, Y, and Er phases required successively greater reaction times. Furthermore, under similar reaction conditions, we have been unable to prepare the Tm, Yb, and Lu phases, despite the fact that $LuCu_2O_4$ has been synthesized previously by solid-state reaction at high oxygen pressures.[2,15]

One explanation for the differences in the rate and amount of product formation is that the solubility of Ln_2O_3 decreases as the size of the Ln^{3+} ion decreases. This reduced solubility can be observed in the Dy, Ho, Y, and Er melts. After a day or so, these melts are not deeply colored but are transparent blue, with undissolved reactants at the bottom of the crucible.

If this is indeed true, then one way to improve the solubility of the smaller, more electropositive cations is to make the melts containing them wetter. Preliminary work indicates that flowing wet air over the melt does improve the yield of $DyCu_2O_4$ in the equimolar melt with a 1-day reaction time from about 1% to 70%. There is also evidence to suggest increased solubility of Ho_2O_3, Y_2O_3, and Er_2O_3 under these conditions.

In early attempts to solve the solubility problem of the smaller rare-earth oxides, we experimented with using $LnCl_3$ and $CuCl_2$ as starting reagents. There was a significant difference in the behavior of these reactants in the hydroxide melts. In general, reactions using chloride starting reagents produced higher yields in oxidizing but relatively dilute melts. However, except in a couple of instances, we did not achieve better results using the halides, so we have not reported their use in this publication.

Table 4. Temperature vs Addition Time, % Yield, and Silver Contamination (Example: $NdCu_2O_4$)[a]

temp (°C)	addition time (h)	% yield	silver impurity
300	6	0	n.a.
350	4	45	none
370	4	60	some
380	4	60	some
380	6	75	none
380	9.5	50	none
400	6	60	lots
400[b]	6	90	none
450	6	0	n.a.

[a] Reactions in 12 g of equimolar melt overnight, using a stoichiometric amount of oxide reagents (CuO = 0.100 g). [b] Dry $Nd(OH)_3$.

Temperature and Addition Time. The reaction temperature and the time before the addition of the starting reagents were adjusted during the course of these investigations. As indicated in Table 4 for the specific case of $NdCu_2O_4$, although trace amounts of $NdCu_2O_4$ were synthesized even at 300 °C, it was necessary to raise the temperature above about 350 °C for $NdCu_2O_4$ to be the dominant phase; at temperatures below 300 °C, the starting materials remained unreacted. Because the water content varied dramatically over the first several hours at a given reaction temperature, the reactant addition time was found to be a key variable. If the reactants were added to a melt that is not dry enough, the Cu(II)-containing oxide, Nd_2CuO_4, precipitated instead of the $NdCu_2O_4$ product. Nd_2CuO_4 also formed at temperatures above 400 °C. In addition, if the reactants were added to a melt that was too wet, the silver crucible was etched, and consequently, silver was obtained as an impurity in the final product.

As shown in Table 4 specifically for $NdCu_2O_4$, variations in temperature and reagent addition time resulted in changes in yield and in the amount of silver contamination. A minimum of 4 h was required before the addition of the reagent oxides in order to form $NdCu_2O_4$ (instead of Nd_2CuO_4). Increasing the temperature from 350 °C increased the yield, but the products contained a small amount of silver. By waiting longer until adding the reagent oxides to the melt (6 h), or by drying the $Nd(OH)_3$ at 200 °C overnight before use, the silver impurity phase disappeared. For longer times before addition of reagents, the yield and the crystal quality decreased.

Two additional approaches were considered with regards to eliminating silver from the product: choosing a different crucible or selectively dissolving the silver in the product. Unfortunately, there were very few alternatives to contain hydroxide melts. In nickel, alumina, and Teflon crucibles, $LnCu_2O_4$ did not form without at least a strip of silver metal present, and then $LnCu_2O_4$ formed in low yields and formed only on the silver. It is possible to remove the silver impurity from the product by washing first in 6 M HCl and then in 12 M NH_4OH; $LnCu_2O_4$ is not soluble in either of these solutions. Although this resulted in pure $LnCu_2O_4$, it

is notable that the crystal quality of products containing silver was consistently poorer as determined visually and by X-ray diffraction, even before treatment to remove the silver. Therefore, it was important to avoid melt conditions that lead to etching of the silver crucible by varying the temperature and reactant addition time.

The problem with silver contamination varied in severity depending on the lanthanide element used. The lanthanides with the most significant problems were Nd and Sm. If the lanthanide oxides used in the synthesis of these analogues were not dried sufficiently prior to addition to the melt, lower temperatures were required to avoid silver contamination. In addition, there was a clear trend that the melts needed to be drier before reagent addition as the reaction temperature increased.

It is known that silver dissolves in very wet melts if the oxidation potential is high enough.[16] Increasing the temperature increases the oxidation potential of the melt, and therefore, silver contamination is more of a problem at higher temperatures, particularly in wet melts. Due to the fine particle size of lanthanide oxides, they typically contain large amounts of adsorbed water. This adsorbed water can dissolve in the melt much more quickly than the oxides, making the melts temporarily wet enough to dissolve silver. Therefore, it is important to dry the Ln_2O_3 starting reagent and wait a sufficient amount of time before addition.

Results and Discussion: Structure

Since we were unable to obtain single crystals for analysis by X-ray diffraction, the structures of the $LnCu_2O_4$ phases were determined by profile refinement of powder X-ray diffraction data. Representative patterns of these phases are presented in Figure 2. Atom positions, isotropic thermal parameters, and refinement statistics for the various $LnCu_2O_4$ phases are listed in Table 5. The final *R* factors and the values of the reduced χ^2 reported here are a statistical measure of the goodness of fit of the structural model to the observed X-ray diffraction data. As these values are quite reasonable for powder X-ray diffraction data, these Rietveld refinements confirm that all members of the series are isostructural.

A view of the monoclinic unit cell of $LnCu_2O_4$ is shown in Figure 1. There are two crystallographically distinct sites for copper in the unit cell, labeled as Cu(1) and Cu(2), two distinct sites for oxygen, and one unique site for the lanthanide ion. The lattice parameters (space group *I*2/*a*) and cell volume are given in Table 6, and selected bond lengths are given in Tables 7 and 8 for each of the $LnCu_2O_4$ phases that were obtained. The systematic variations that are observed with the size of the lanthanide ion are discussed below.

The lanthanide atoms are located in a distorted square antiprismatic array of oxygen atoms (four O(1) and four O(2) atoms). Each LnO_8 polyhedron is linked to three other LnO_8 polyhedra via edges, one edge containing two O(2) atoms, the other edges containing two O(1) atoms. These linked polyhedra form a three-dimensional array shown in Figure 3. The average observed Ln−O bond distances are in good agreement with those calculated with the Shannon−Prewitt radii[17] as shown in Table 7. The decrease in the Ln−O bond lengths is correlated linearly with a decrease in the radius of the Ln^{3+} ion and unit cell volume. Ln−Ln distances tend to be about 0.15 Å longer than those in Ln_2CuO_4 and are at least 0.1 Å longer than those found in the elemental metal.

Each copper atom is surrounded by two O(1) and two O(2) atoms in a distorted square-planar arrangement,

Table 5. Atom Positions, Isothermal Temperature Factors, and Refinement Statistics[a]

$LnCu_2O_4$	atom	*x*	*y*	*z*	$100U_{iso}$	refinement statistics
La	La	0.25	0.1242(3)	0	4.2(1)	$R_p = 0.0760$
	Cu(1)	0.75	0.25	0.75	3.8(2)	$R_{wp} = 0.0962$
	Cu(2)	0	0.5	0	3.3(2)	$\chi^2 = 1.214$
	O(1)	0.528(2)	0.833(1)	0.614(2)	6.5(4)	
	O(2)	0.902(2)	0.073(1)	0.218(2)	3.3(4)	
Nd	Nd	0.25	0.1247(2)	0	3.3(1)	$R_p = 0.0797$
	Cu(1)	0.75	0.25	0.75	2.7(2)	$R_{wp} = 0.1002$
	Cu(2)	0	0.5	0	2.8(2)	$\chi^2 = 1.211$
	O(1)	0.538(2)	0.837(1)	0.624(2)	2.1(4)	
	O(2)	0.892(2)	0.077(1)	0.208(2)	1.1(4)	
Sm	Sm	0.25	0.1252(3)	0	3.1(1)	$R_p = 0.0827$
	Cu(1)	0.75	0.25	0.75	3.2(2)	$R_{wp} = 0.1052$
	Cu(2)	0	0.5	0	2.5(2)	$\chi^2 = 1.092$
	O(1)	0.532(2)	0.834(2)	0.632(2)	2.9(5)	
	O(2)	0.902(2)	0.072(1)	0.207(2)	1.9(5)	
Eu	Eu	0.25	0.1250(3)	0	3.3(1)	$R_p = 0.0819$
	Cu(1)	0.75	0.25	0.75	3.0(2)	$R_{wp} = 0.1033$
	Cu(2)	0	0.5	0	2.4(2)	$\chi^2 = 1.131$
	O(1)	0.534(2)	0.831(1)	0.632(2)	3.2(4)	
	O(2)	0.899(2)	0.076(1)	0.205(2)	2.5(4)	
Gd	Gd	0.25	0.1263(3)	0	2.7(1)	$R_p = 0.0806$
	Cu(1)	0.75	0.25	0.75	2.1(2)	$R_{wp} = 0.1016$
	Cu(2)	0	0.5	0	2.9(2)	$\chi^2 = 1.171$
	O(1)	0.540(2)	0.827(1)	0.620(2)	2.5	
	O(2)	0.889(2)	0.076(1)	0.206(2)	2.5	
Dy	Dy	0.25	0.1246(3)	0	2.9 (1)	$R_p = 0.0821$
	Cu(1)	0.75	0.25	0.75	2.5(1)	$R_{wp} = 0.1028$
	Cu(2)	0	0.5	0	1.9(1)	$\chi^2 = 1.214$
	O(1)	0.541(2)	0.832(1)	0.620(2)	0.6(3)	
	O(2)	0.901(2)	0.075(1)	0.206(2)	2.5	
Ho	Ho	0.25	0.1251(2)	0	4.1(1)	$R_p = 0.0643$
	Cu(1)	0.75	0.25	0.75	2.8(1)	$R_{wp} = 0.0832$
	Cu(2)	0	0.5	0	2.3(1)	$\chi^2 = 1.461$
	O(1)	0.543(1)	0.828(1)	0.628(1)	2.3(2)	
	O(2)	0.900(1)	0.077(1)	0.206(1)	2.5(3)	
Y	Y	0.25	0.1252(2)	0	6.3(1)	$R_p = 0.0617$
	Cu(1)	0.75	0.25	0.75	5.0(1)	$R_{wp} = 0.0767$
	Cu(2)	0	0.5	0	5.0(1)	$\chi^2 = 1.551$
	O(1)	0.533(1)	0.836(1)	0.632(1)	5.1(3)	
	O(2)	0.897(1)	0.071(1)	0.196(1)	3.2(3)	
Er	Er	0.25	0.1267(2)	0	6.3(1)	$R_p = 0.0868$
	Cu(1)	0.75	0.25	0.75	4.6(1)	$R_{wp} = 0.1112$
	Cu(2)	0	0.5	0	3.9(1)	$\chi^2 = 1.477$
	O(1)	0.563(2)	0.815(1)	0.634(2)	3.5(4)	
	O(2)	0.907(1)	0.069(1)	0.199(2)	2.0(3)	

[a] Parameters without errors are not refined.

Table 6. Lattice Parameters of $LnCu_2O_4$

$LnCu_2O_4$	*a* (Å)	*b* (Å)	*c* (Å)	β (deg)	V (Å^3)
La	5.9219(2)	9.7677(3)	5.8489(2)	92.243(1)	338.06(3)
Nd	5.8250(3)	9.6975(4)	5.7532(2)	92.276(2)	324.73(4)
Sm	5.7813(3)	9.6581(5)	5.7062(3)	92.305(2)	318.36(4)
Eu	5.7638(3)	9.6422(4)	5.6864(3)	92.350(2)	315.76(4)
Gd	5.7460(3)	9.6259(4)	5.6709(3)	92.317(2)	313.40(4)
Dy	5.7049(3)	9.5912(4)	5.6248(3)	92.448(2)	307.49(4)
Ho	5.6871(1)	9.5722(2)	5.6093(1)	92.454(1)	305.08(1)
Y	5.6867(3)	9.5723(4)	5.6062(3)	92.460(1)	304.89(4)
Er	5.6716(1)	9.5567(2)	5.5943(1)	92.436(1)	302.95(1)

(14) Plembeck, J. A. In *Encyclopedia of Electrochemistry of the Elements*; Bard, A. J., Ed.; *Fused Salt Systems*; Marcel Dekker, Inc.: New York 1976, Vol. X, pp 285−9.

(15) We have also been unsuccessful in synthesizing the Ce, Pr, and Tb analogues in these melts. We believe that this is because these lanthanides convert to their 4+ oxidation state in the molten hydroxides and thus cannot be incorporated into the $LnCu_2O_4$ structure.

(16) Goret, J.; Tremillion, *Electrochim. Acta* **1967**, *12*, 1065.

(17) Shannon, R. D. *Acta Crystallogr.* **1974**, *A32*, 751.

Table 7. Selected Ln−O and Ln−Ln Bond Distances[a]

$LnCu_2O_4$	Ln−O(1)	Ln−O(2)	average Ln−O	Ln−O[b]	Ln−Ln	Ln−Ln[c]
La	2.53(1), 2.60(1)	2.46(1), 2.52(1)	2.53(6)	2.54	3.820(3), 3.828(3)	3.76
Nd	2.48(1), 2.51(1)	2.42(1), 2.49(1)	2.48(4)	2.49	3.765(4), 3.786(3)	3.64
Sm	2.44(1), 2.51(1)	2.39(1), 2.43(1)	2.44(5)	2.46	3.736(4), 3.768(4)	3.60
Eu	2.43(1), 2.48(1)	2.40(1), 2.42(1)	2.43(3)	2.45	3.728(4), 3.757(4)	3.60
Gd	2.39(1), 2.47(1)	2.39(1), 2.47(1)	2.43(5)	2.43	3.703(4), 3.763(4)	3.60
Dy	2.39(1), 2.45(1)	2.38(1), 2.40(1)	2.41(3)	2.41	3.701(3), 3.722(3)	3.54
Ho	2.39(1), 2.40(1)	2.39(1), 2.39(1)	2.39(2)	2.40	3.685(2), 3.718(2)	3.54
Y	2.39(1), 2.49(1)	2.32(1), 2.39(1)	2.40(7)	2.40	3.683(3), 3.719(3)	3.60
Er	2.23(1), 2.34(1)	2.34(1), 2.35(1)	2.32(6)	2.38	3.658(3), 3.730(3)	3.52

[a] All distances are in angstroms. [b] Calculated using Shannon−Prewitt radii. [c] Calculated using metallic radii.

Table 8. Selected Cu−O and Cu−Cu Bond Distances[a]

$LnCu_2O_4$	Cu(1)−O(1)	Cu(1)−O(2)	average Cu(1)−O	Cu(2)−O(1)	Cu(2)−O(2)	average Cu(2)−O	Cu(1)−Cu(1)	Cu(2)−Cu(2)
La	2.02(1)	1.96(1)	1.99(4)	1.77(1)	1.87(1)	1.82(7)	2.9244(1)	2.9606(1)
Nd	2.04(1)	1.89(1)	1.97(11)	1.75(1)	1.92(1)	1.84(12)	2.8766(1)	2.9125(1)
Sm	1.97(1)	1.95(1)	1.96(1)	1.77(1)	1.88(1)	1.83(8)	2.8531(1)	2.8907(1)
Eu	1.96(1)	1.91(1)	1.94(4)	1.80(1)	1.90(1)	1.85(7)	2.8432(1)	2.8819(1)
Gd	1.99(1)	1.88(1)	1.94(8)	1.81(1)	1.91(1)	1.86(7)	2.8354(1)	2.8730(1)
Dy	1.98(1)	1.91(1)	1.95(5)	1.79(1)	1.86(1)	1.83(5)	2.8124(1)	2.8524(1)
Ho	1.97(1)	1.89(1)	1.93(6)	1.81(1)	1.87(1)	1.84(4)	2.8047(1)	2.8435(1)
Y	1.95(1)	1.94(1)	1.95(1)	1.74(1)	1.91(1)	1.83(12)	2.8031(1)	2.8433(1)
Er	2.01(1)	1.97(1)	1.99(3)	1.95(1)	1.87(1)	1.91(6)	2.7972(1)	2.8358(1)
		total ave = 1.96(5)			total ave = 1.84(6)			

[a] All distances are in Å. Typical bond distances are: Cu^{2+}−O, 1.96 Å (CuO); Cu^{3+}−O, 1.85 Å;[5] Cu−Cu, 2.56 Å (Cu metal).

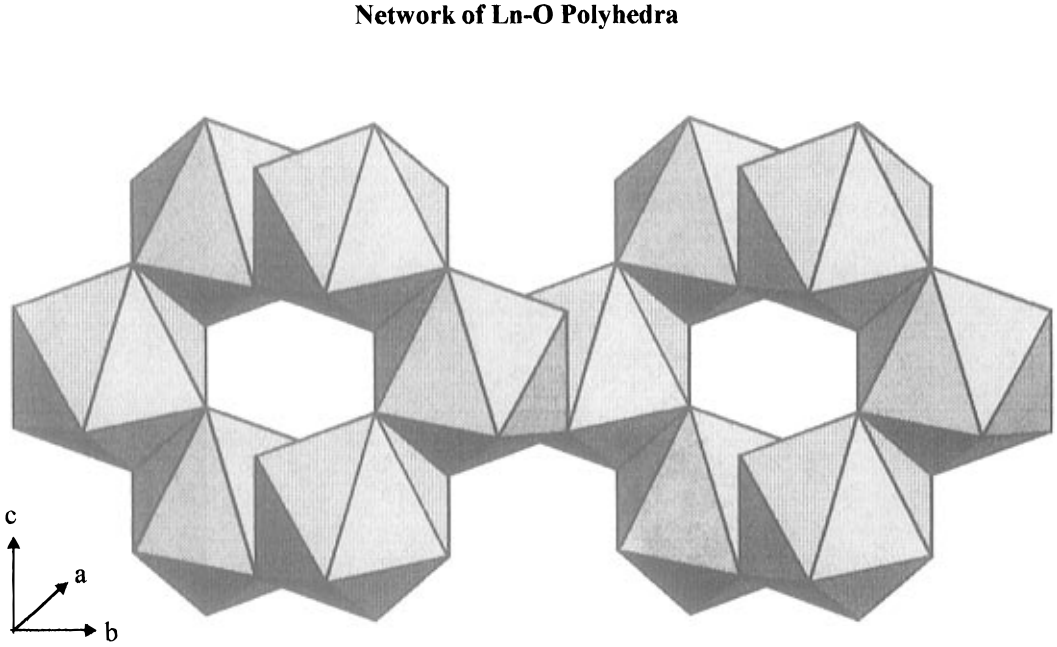

Figure 3. Network of Ln−O polyhedra.

and the units are corner-shared in a three-dimensional array which interpenetrates and is linked to the Ln−O network through both corner- and edge-sharing. The average Cu−O bond lengths are quite different for Cu(1) and Cu(2) as indicated in Table 8. The average Cu(1)−O bond distances observed are typical for Cu^{2+} (e.g., in CuO: Cu−O = 1.96 Å[18]), whereas the average Cu(2)−O bond distances observed are typical for Cu^{3+} (e.g., in $Ba_4NaCuO_4(CO_3)_2$: Cu−O = 1.85 Å[5]). Unlike in the case of the Ln−O bond distances, there appears to be no correlation of the Cu−O bond distances with the size of the Ln^{3+} ion. This conclusion is also supported by preliminary powder neutron data on the La and Y analogues.

The $Cu(1)O_4$ units are stacked above each other along the *c* direction, and the $Cu(2)O_4$ units are stacked along the *a* direction in such a way that the copper atoms form widely spaced chains. The Cu−Cu distances are also listed in Table 8. The separation between the copper atoms (2.80−2.96 Å) is significantly longer than bond lengths found in the elemental metal (2.56 Å). This indicates that there is probably no significant bonding between the copper atoms in the chain, though there could still be other types of interactions (i.e., magnetic). It is notable that the Cu^{2+}−Cu^{2+} distances (2.80−2.92 Å) are generally about 0.04 Å shorter than the Cu^{3+}−Cu^{3+} distances (2.84−2.96 Å). Both decrease with decreasing cell volume.

The oxygen atoms are coordinated to two lanthanide ions and two copper ions in a distorted tetrahedral

(18) Wells, A. F. *Structural Inorganic Chemistry*, 5th ed.; Oxford: Clarendon Press, 1984; p 1120.

array. Since the oxygen atoms are on general positions, we allowed the coordinates for the oxygen atoms to vary. Additionally, we varied the *y*-coordinate of the lanthanide atoms. As shown in Tables 7 and 8, the resulting Ln−O and Cu−O coordination environments were quite distorted. This was also true for the Nd analogue, even though previous refinement of neutron diffraction data did not show these distortions. Since the neutron-scattering factor for oxygen is significantly larger than the X-ray scattering factor, the oxygen positions obtained from the neutron experiment are more accurate. Therefore, it seems that in order to get more accurate oxygen atom positions, and thereby more accurate bond lengths and angles, additional neutron data should be collected on this system. This work is in progress.

Conclusions

The synthesis of $LnCu_2O_4$ has been a valuable means by which to probe different synthetic conditions in the molten hydroxides. Increasing the ratio of KOH to NaOH increases the acidity and the stability of higher oxidation states of Cu, generally favoring the formation of $LnCu_2O_4$. Greater yields of $LnCu_2O_4$ are generally obtained in the more concentrated melts with high activities of O^{2-}. However, there are obstacles in the synthesis of the smaller lanthanide analogues. This is probably a result of decreased solubility of Ln_2O_3. There is also a problem with the larger rare earths (especially Nd, Sm) with the contamination of the $LnCu_2O_4$ product by silver. This can be attributed to increased acidity of the hydroxide melts due to the dissolution of adsorbed water from the Ln_2O_3, which leads to etching of the silver crucible. The etching can be reduced by drying the Ln_2O_3 reactant before use and increasing the time between the start of the experiment and the addition of the oxide reagents.

We have also observed a number of structural trends. The average Ln−O distances remain in good agreement with bond distances calculated using Shannon−Prewitt radii,[17] and the average Cu−O distances are in good agreement with previously published data.[5,18] Since there is some uncertainty as to the accuracy of the oxygen positions obtained, it will be necessary to collect neutron data on these analogues in order to better resolve these atom positions.

Acknowledgment. This work was supported by the National Science Foundation (Grant DMR-9417185). J.L.L. is grateful to the National Science Foundation for a Graduate Research Fellowship.

CM960226U